Structural Eng. / Earthquake Eng. Vol. 5. No. 2, 235s- 243s. October 1988
Japan Society of Civil Engineers (Proc. of JSCE No. 398/I-10)

A PARAMETRIC STUDY ON FATIGUE DESIGN CURVES FOR STEEL HIGHWAY BRIDGES

By Chitoshi MIKI, Masahiro SAKANO** and Jun MURAKOSHI****

Fatigue design curves of steel highway bridges were analyzed parametrically under computer simulated variable amplitude stresses. Crack propagation life of 4 types of welded joints was estimated by applying the constant amplitude da/dN-ΔK relationship and the liner cumulative damage rule. The configuration of fatigue life curves under variable amplitude stresses varied with the traffic constitution and the beam span particularly in the longer life region. The fatigue limit under variable amplitude stresses for each joint could be defined by using estimated fatigue life curves and Miner's rule.

Keywords : fatigue analysis, highway bridge, design curve

1. INTRODUCTION

In recent years, fatigue cracking has appeared in various parts of steel highway bridges in Japan[1),2)]. As a means of investigation into the causes of cracking, the long-term measurement of actual stresses has been carried out[3),4)]. The actual stress range histogram obtained through such measurement is extremely inclined to the low-stress side. Therefore, in order to evaluate the fatigue life of steel bridge members effectively, it is essential to study the fatigue behavior under variable amplitude stresses with such a stress range histogram. Fisher et al.[5)] indicated that fatigue cracks developed under variable amplitude stresses even though most of the stress ranges were well below the constant amplitude fatigue limit. It is, therefore, of great importance how to deal with the lower stress ranges in variable amplitude stresses for assessment of fatigue damage of steel bridge members.

In the Japanese standard for the design of steel railway bridges[6)], the correction factor for the effect of variable amplitude stresses is calculated using the modified Miner's rule and design curves of the fixed slope for each of the following : $-1/3$ for heat treated steel welded joints, $-1/4$ for non-heat treated steel welded joints and $-1/5$ for non-welded joints. When applied under variable amplitude stresses with such extremely large frequency of lower stress ranges as occurring in highway bridges, however, the modified Miner's rule is too conservative because of overestimating the cumulative fatigue damage by lower stress cycles. In standard specifications for fatigue design of steel highway bridges or other steel structures in

* Member of JSCE, Dr. Eng., Associate Professor, Department of Civil Engineering, Tokyo Institute of Technology (O-okayama, Meguro-ku, Tokyo)
** Member of JSCE, Dr. Eng., Research Associate, Department of Construction Engineering, Gunma University (Kiryu-shi, Gunma)
*** Member of JSCE, M. Eng., Research Engineer, Public Work Research Institute, Ministry of Construction (Tsukuba-shi, Ibaragi)

foreign countries, Miner's rule is generally used for accurate evaluation of the fatigue life under variable amplitude stresses. In that case, if applied on the basis of the constant amplitude fatigue limit, Miner's rule is unsafe because of disregarding the fatigue damage by stress cycles lower than the fatigue limit. Therefore, the configuration of design curves in the longer life region is contrived in each of those specifications. The slope of design curves is changed from $-1/3$ to $-1/5$ at the number of stress cycles $N=10^7$ in BS5400[7], from $-1/3$ to $-1/5$ at $N=5\times10^6$ and to horizontal at $N=10^8$ in ECCS recommendations[8], and from about $-1/3$ to horizontal at different N for each category in AASHTO specifications[9]. Consequently, in order to evaluate the fatigue life of highway bridge members in Japan applying Miner's rule with sufficient accuracy, it is necessary to define fatigue design curves in which the characteristics of actual stresses are adequately reflected. It is, however, practically impossible to define the design curve through long life fatigue tests on all kinds of details under various stress fluctuations supposed to occur in highway bridges.

In a previous experimental study[10] on the crack propagation behavior under computer simulated highway variable loading, the authors confirmed that the fatigue crack growth threshold stress intensity factor range ΔK_{th} exists in a similar way as under constant amplitude loading, and that it is possible to estimate the fatigue crack growth rate with adequate accuracy by applying the constant amplitude da/dN-ΔK relationship and the linear cumulative damage rule to ΔK exceeding ΔK_{th}. In this study, parametric analyses on fatigue life curves are carried out, based on the fatigue crack propagation life under various stress fluctuations supposed to occur in highway bridges, and the fatigue limit level used to evaluate the fatigue life by applying Miner's rule and the fatigue design curve consisting of a slanting line and a fatigue limit is investigated.

2. VARIABLE AMPLITUDE STRESSES USED IN ANALYSES

In this study, in order to deal with various types of variable amplitude stresses supposed to occur in highway bridges, bending moment fluctuations arising at the center of a simple beam span when a column of vehicles generated by computer simulations[11] passes over are used as stress fluctuations in fatigue life analyses. An example of simulated moment history is shown in Fig. 1. The traffic simulation models consist of three types, which are given in Table 1. Models ① and ② simulate respectively the traffic flow with an extremely high percentage of large trucks which occurs during the night and that occurring usually during the daytime on the Tohmei Expressway. Model ③ simulates a traffic flow with a high percentage of cars on an urban expressway such as the Tokyo Metropolitan Expressway or the Hanshin Expressway. The simple beam spans are 10, 50 and 100 m.

Maximum (M_{max}) and equivalent ($M_{eq}=(\sum_{i=1}^{N} M_i^3/N)^{1/3}$) ranges of nine types of moment fluctuations obtained by simulations of 20 000 vehicles and their ratio (M_{eq}/M_{max}) are given in Table 2. Fig. 2 shows the cumulative distributions of non-dimensional stress ranges for each span. As the percentage of large trucks decreases and the span becomes longer, M_{eq}/M_{max} is smaller and the proportion of the lower stress ranges becomes larger.

In Fig. 2, cumulative distributions of stress ranges measured for 24 hours at the lower flange and the top end of the vertical stiffener in three plate girder bridges are shown together. Bridges K and T are the non-composite two-span continuous bridge of a 20 m span with a large truck percentage of 40, and Bridge A is a simply-supported live-load-composite bridge of a 42 m span with a large truck percentage of 24. The actual stress range distributions in Bridges K and T are so close to the distribution of model ② (the large truck percentage is 45) for a 10 m span, and because those in Bridge A lie in between model ② and ③ (the large truck percentage is 13) for a 50 m span, that it may be said that the computer simulated variable stresses used in these analyses cover a wide range of actual stress fluctuations occurring in various highway bridge members. Consequently, it is amply sufficient to deal with such stress fluctuations as these in order to establish the fatigue design curves for highway bridge members.

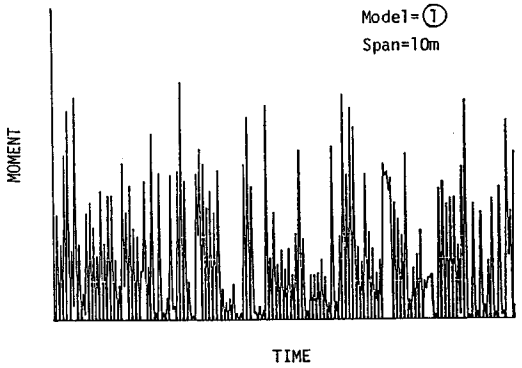

Fig. 1 An Example of Simulated Moment Fluctuations.

Table 1 Vehicle Type Percentages of Simulation Traffic Models.

Traffic model	①	②	③
Car	10	50	75
Small truck	5	5	12
2 axes large truck	25	20	10
3 axes large truck	50	20	2
4 axes trailer	10	5	1

Table 2 Maximum and Equivalent Moment Ranges of Simulation Loadings.

Span (m)	Traffic model	Mmax (tonf·m)	Meq	Meq/Mmax
10	①	130	36	0.278
	②	100	28	0.278
	③	80	16	0.203
50	①	990	253	0.255
	②	990	192	0.194
	③	670	102	0.153
100	①	2440	610	0.250
	②	2270	462	0.203
	③	1780	240	0.135

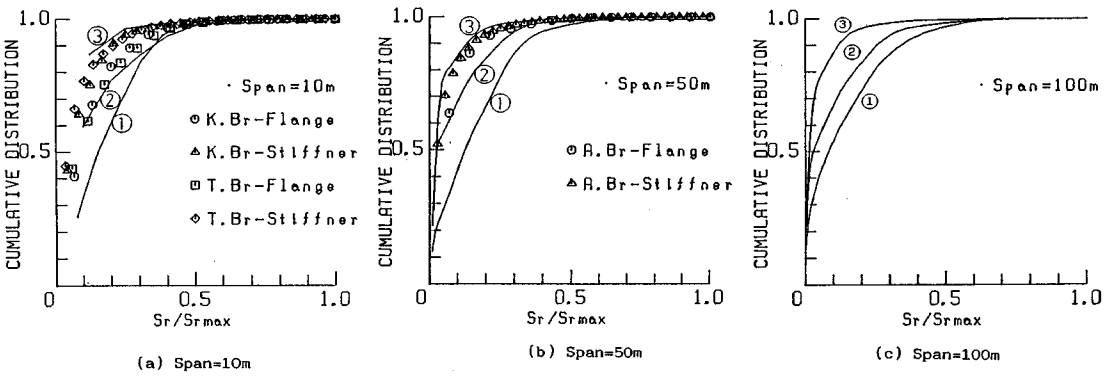

(a) Span=10m (b) Span=50m (c) Span=100m

Fig. 2 Cumulative Distributions of Variable Amplitude Stress Ranges.

3. PROCEDURES OF ANALYSES

Fatigue life analyses are carried out on the welded joints typical of fatigue categories (A, B, C and D) of the Japanese standard for the design of steel railway bridges[6]. These consist of the four types of butt joint (BT), flange gusset joints (FG, R=40 mm and R=20 mm) and stiffener joint (ST) as shown in Fig. 3. The thickness and width of the main plate are 30 mm and 200 mm for each joint. As to the ST joint, taking account of the thickness effect[12], the plate thicknesses of 45 mm and 75 mm allowed for use in Honshu-Shikoku Bridges[13] are added.

The stress intensity factor range ΔK is determined by Eq. (1).

$$\Delta K = F_e \cdot F_s \cdot F_t \cdot F_g \cdot S_r \sqrt{\pi a} \quad \cdots\cdots (1)$$

Where, S_r is nominal stress range on the minimum area, a is crack depth. F_e, F_s, F_t and F_g are correction factors to account for effects of crack shape, free surface, finite thickness or width, and stress concentration respectively.

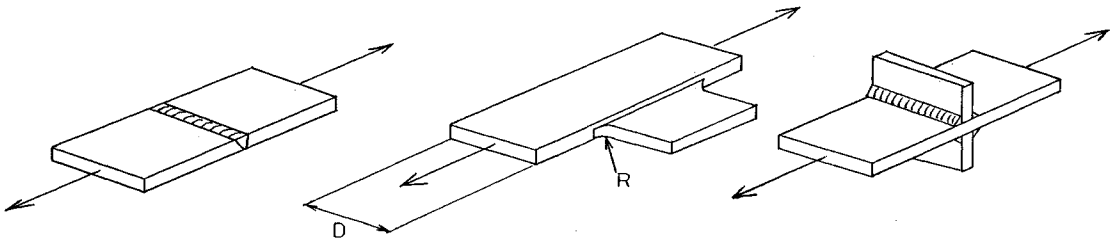

(a) Butt Joint (BT) (b) Flange Gusset Joint (FG) (c) Stiffener Joint (ST)

Fig. 3 Welded Joints for Analyses.

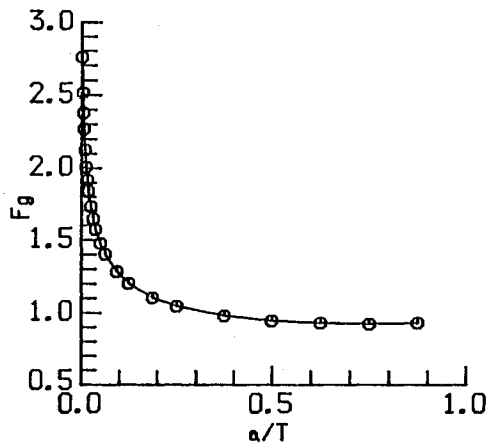

Fig. 4 Relationship between F_g and a/T for Stiffener Joint.

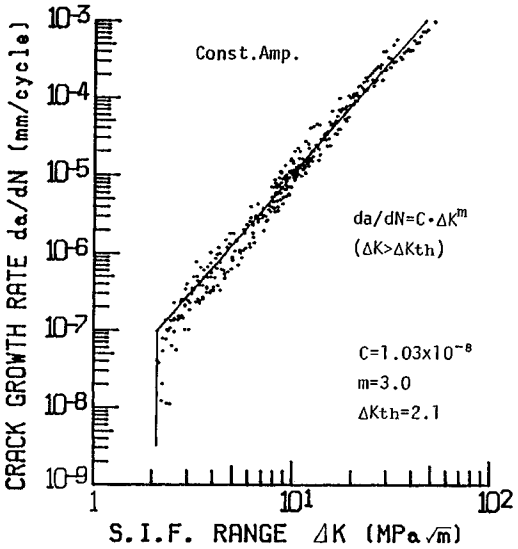

Fig. 5 Relationship between da/dN and ΔK under Constant Amplitude Loading[10].

In these analyses, because of assuming semi-circular surface cracks, $F_e=2/\pi$, $F_s=1$, and F_t is given by Eq. (2)[14].

$$F_t=(1-0.025\,\lambda^2+0.06\,\lambda^4)\sqrt{\sec(\pi\lambda/2)} \quad \cdots\cdots (2)$$

where, $\lambda=a/T$, T is plate thickness.

F_g is equal to 1 for BT Joint since no stress-concentration occurs, and is calculated by Eq. (3) after Fisher et al.[15] for FG Joint.

$$F_g=\frac{-1.115\log(R/W_f)+0.5370\log(L/W_f)+0.1384\log(W_{gp}/W_f)+0.6801}{1+1/1.158\,\alpha^{0.6051}} \quad \cdots\cdots (3)$$

where, R is fillet radius, L is gusset plate length plus twice of R, W_f is flange (main plate) width, W_{gp} is gusset plate width, and α equals a/W_f.

F_g for ST joint is calculated as the stress intensity factor for an edge crack in a semi-infinite plane subjected to the distributed stresses occurred without the crack[14]. The stress distribution is obtained by the finite elements analysis on the assumption of a 135 dig. flank angle and a 0.75 mm toe radius. Fig. 4 shows the distribution of F_g in the direction of plate thickness at the weld toe. The relationship between crack growth rate da/dN and stress intensity factor range ΔK under constant amplitude stresses is indicated in Fig. 5 and given by Eq. (4)[10].

$$da/dN=\begin{cases} C\cdot\Delta K^m & (\Delta K>\Delta K_{th}) \\ 0 & (\Delta K\leqq\Delta K_{th}) \end{cases} \quad \cdots\cdots (4)$$

where, $C=1.03\times10^{-8}$, $m=3.0$, and $\Delta K_{th}=2.1\,\mathrm{MPa}\sqrt{m}$.

Fatigue crack propagation life N_p is calculated by Eq. (5), applying Eq. (4) and the liner cumulative damage rule to each range of variable amplitude stresses.

$$N_p=\int_{a_i}^{a_f} da/(C\cdot\Delta K^m) \quad (5)$$

In this case, initial crack radius a_i is fixed at 0.2 mm out of consideration for the under-cut or the grinder-scratch liable to remain in actual welded joints and the correspondence to the fatigue design curve. Final crack radius a_f is assumed to be 80 percent of the plate thickness.

4. RESULTS OF ANALYSES AND CONSIDERATIONS

(1) Configuration of fatigue life curve

Fig. 6 shows the fatigue life curves under constant amplitude stresses. Fatigue life curves become horizontal about 4×10^6 cycles of stress repetition for BT and FG joints, and more than 10^7 cycles for ST joint, where fatigue limits exist corresponding to ΔK_{th}. The constant amplitude fatigue limit of each joint is 131, 98, 81, and 57 MPa. The fatigue life curve for each joint except ST Joint coincides with the fatigue design curve for each category of the Japanese standard for the design of steel railway bridges[6].

Fatigue life curves under simulated variable amplitude stresses of a span 10 m and traffic model ② are shown in Fig. 7. S_{req} as ordinate is the equivalent stress range $(=(\sum_{i=1}^{N} S_{ri}^3/N)^{1/3})$ counted by the rainflow method for variable amplitude stresses. The power index 3 corresponds to the value of m in da/dN vs ΔK relationship used for fatigue life estimation (Eq. (4)). In the shorter life region the fatigue life curves under variable amplitude stresses agree with those under constant amplitude stresses. In the longer life region, however, those curves differ remarkably as they continue to decline even below the constant amplitude fatigue limits.

Fig. 8 and Fig. 9 show the effects of the vehicle composition and beam span on the fatigue life curve of the BT joint. As the percentage of large trucks decreases and as the beam span becomes longer from 10 m to 50 m, the change of the slope of the fatigue life curve under variable amplitude stresses becomes limited, which approaches the design curve of a slope=1/3. There is, however, little difference between the curves of a span 50 m and 100 m. These tendencies correspond to those of M_{eq}/M_{max} given in Table 2, and the difference according to the type of joint cannot be seen.

Fatigue life curves estimated under nine types of variable amplitude stresses given in Table 2 are shown for each joint in Fig. 10. The configuration of those curves varies according to the variations of stress waveforms, and the fatigue limit does not appear as far as $N=5\times10^8$ cycles, even though the slope of the curves becomes somewhat gentler. One way of defining the fatigue design curve is to draw an enveloping

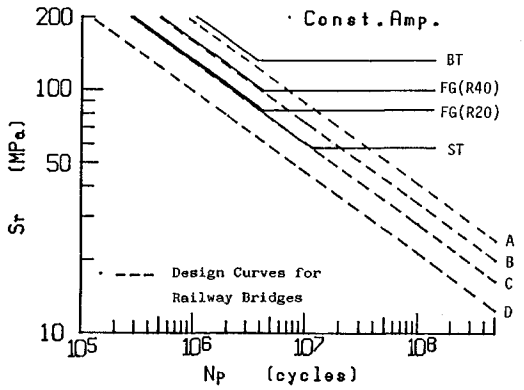

Fig. 6 S_r-N_p Curves under Constant Amplitude Stresses.

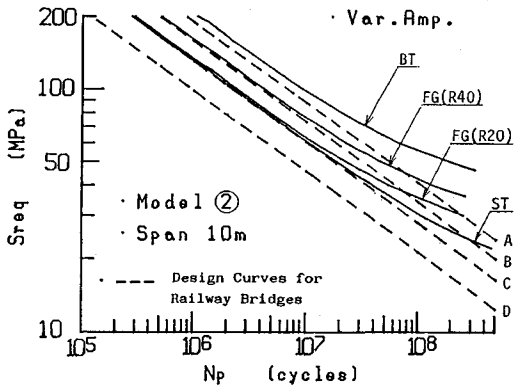

Fig. 7 S_{req}-N_p Curves under Variable Amplitude Stresses.

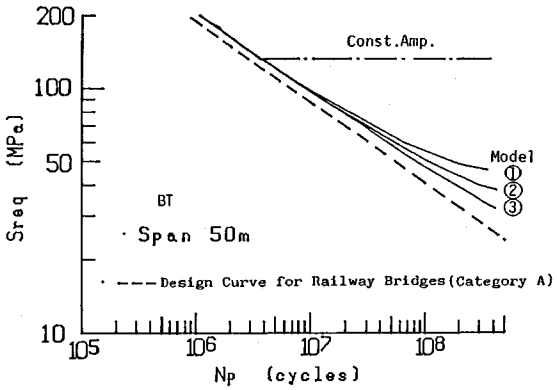

Fig. 8 Effect of Traffic Constitution.

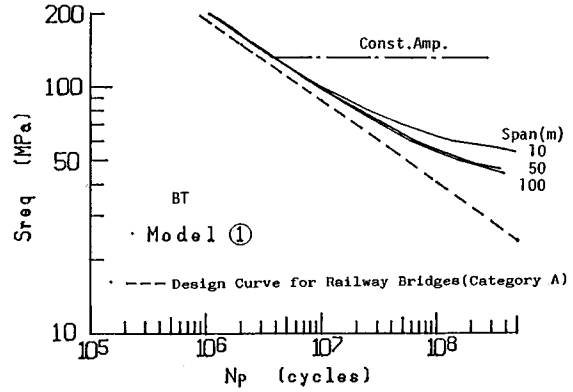

Fig. 9 Effect of Beam Span.

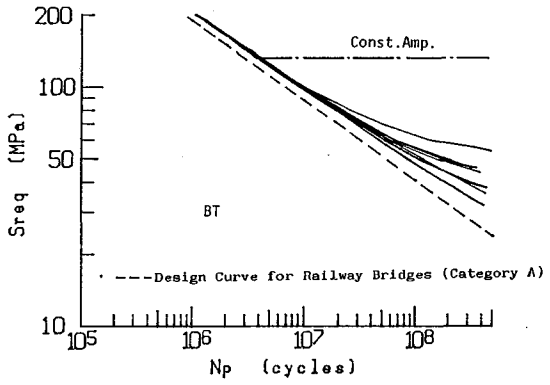

(a) Joint BT

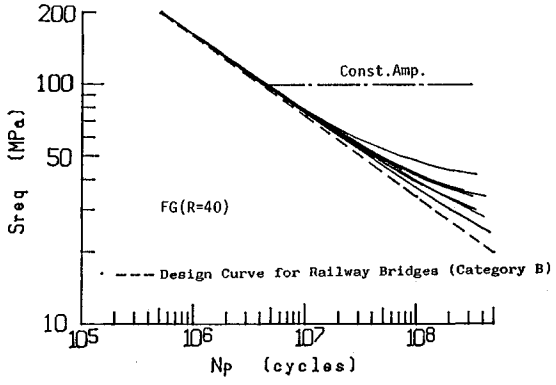

(b) Joint FG (R=40)

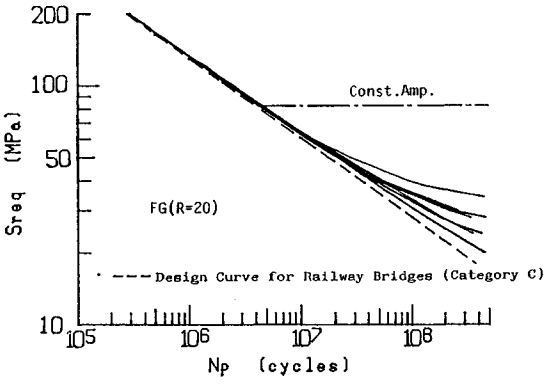

(c) Joint FG (R=20)

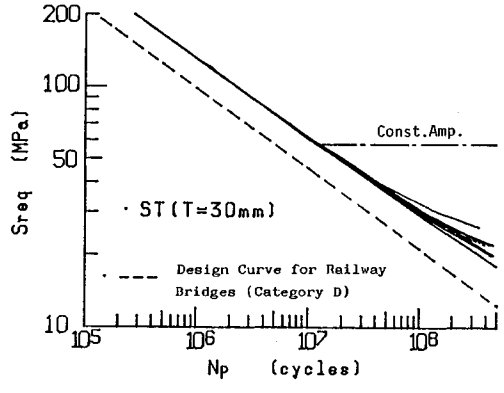

(d) Joint ST (T=30)

Fig. 10 Variation of S_{req}-N_p Curves under Variable Amplitude Stresses.

line of a number of fatigue life curves, however, it is rather difficult to settle the design curve consisting of a slant line and a fatigue limit by that method.

(2) Fatigue limit in design curve

In the fatigue design applying Miner's rule, structural members are designed so that the cumulative damage calculated along the fatigue design curve may be equal to or less than one. In this study, using the fatigue life curves obtained in 4. (1), fatigue limits under variable amplitude stresses are defined conversely so that the Miner's summation may be equal to one.

As shown in Fig. 11, the fatigue limit under variable amplitude stresses is defined as the stress range

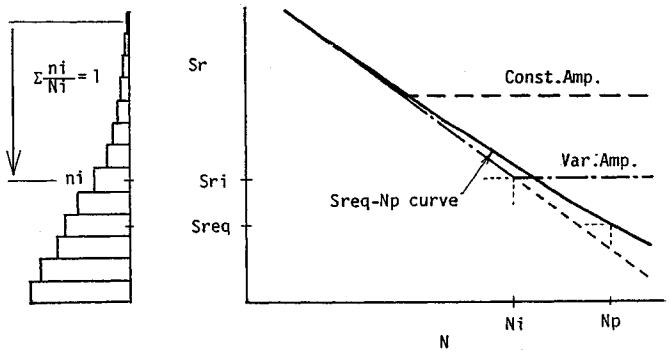

Fig. 11 Estimation of Fatigue Limit under Variable Amplitude Stresses.

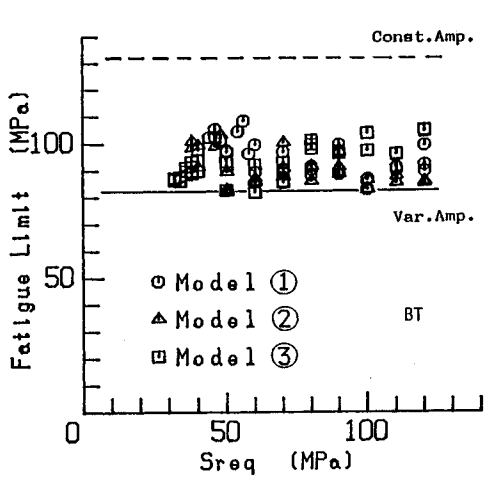

(a) Joint BT

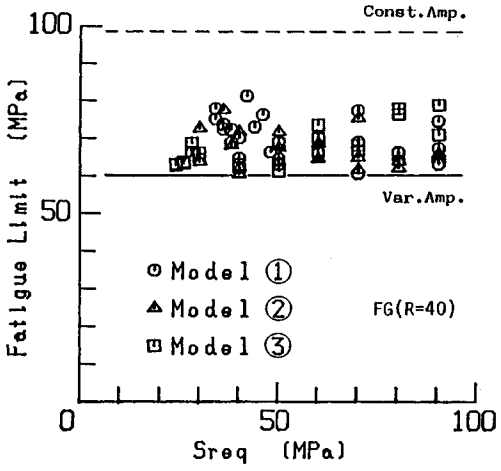

(b) Joint FG (R=40)

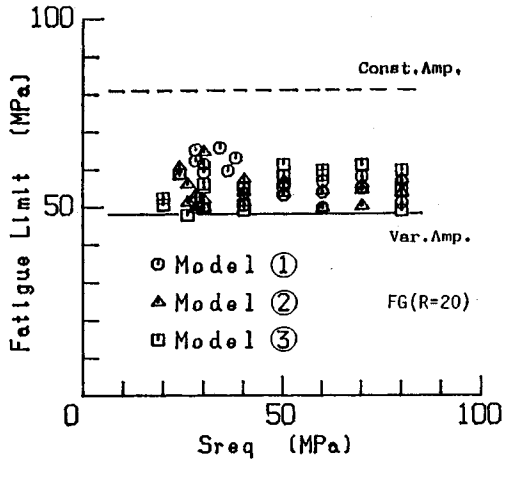

(c) Joint FG (R=20)

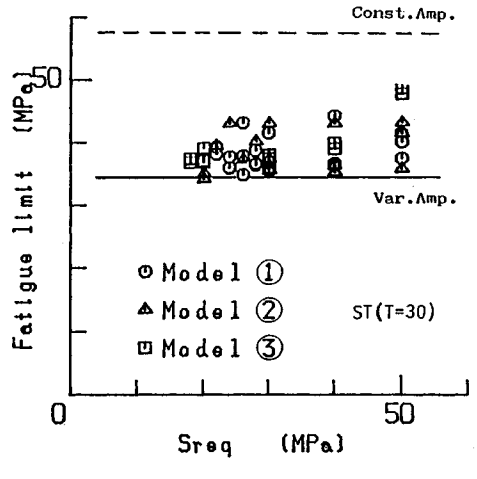

(d) Joint ST (T=30)

Fig. 12 Fatigue Limit under Variable Amplitude Stresses.

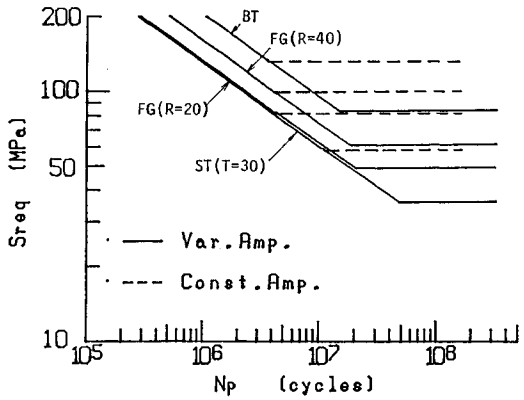

Fig. 13 Fatigue Design Curves under Variable Amplitude Stresses.

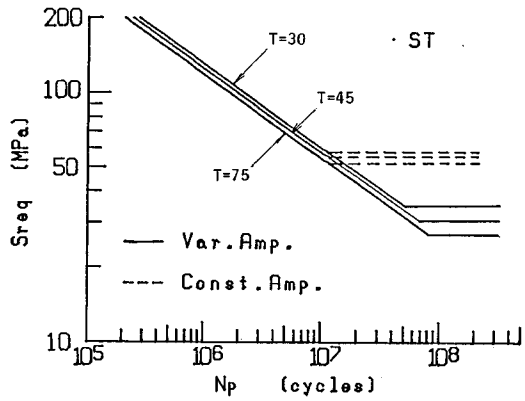

Fig. 14 Effect of Plate Thickness on Fatigue Design Curve for Stiffener Joint.

where the cumulative damage calculated from the high stress side of the stress spectrum with the total frequency of stress cycles equal to the fatigue life estimated under the same stress spectrum reaches one. The fatigue limit of the design curve for each joint can be set up by calculating for various traffic flows and beam spans. S-N relationships used as a basis for counting the cumulative damage are those of fatigue life curves estimated under constant amplitude stresses given by Eq. (6).

$$S_r^m \cdot N = C \quad \cdots\cdots (6)$$

where, $m=3$, C is for each joint, 8.51×10^{12}, 4.07×10^{12}, 2.33×10^{12}, and 1.63×10^{12}.

Stress ranges below the constant amplitude fatigue limit are important in actual bridge members. Fig. 12 shows the relationship between the fatigue limit and the equivalent stress range obtained for each joint by that procedure. Fatigue limits under variable amplitude stresses are generally lower than the constant amplitude fatigue limit shown by the broken line. If Miner's rule is applied on the basis of the constant amplitude fatigue limit, therefore, fatigue life evaluation is unsafe on account of disregarding the fatigue damage by these lower stress ranges. The fatigue limit under each stress waveform is distributed within so narrow a range, independent of the equivalent stress range for each joint (although those of traffic model ① with a comparatively small frequency of lower stress ranges tend to be a little higher), that the fatigue limit under variable amplitude stresses can be defined for each joint by this method. The solid line in Fig. 12 indicates the variable amplitude fatigue limit of 82, 60, 48, and 34 MPa for each joint.

Fatigue design curves consisting of a slanting line and a fatigue limit obtained in this way are shown in Fig. 13. Fatigue life evaluation applying the modified Miner's rule is too conservative because the fatigue damage by stress cycles beneath these fatigue limits is counted. Fig. 14 shows the fatigue design curves obtained by the same method for ST joints with the thickness of 30, 45 and 75 mm. The size effect appears so conspicuously on this type of welded joint; the fatigue limit for the thickness of 45 mm and 75 mm decreases to 88% and 80% respectively of that for the thickness of 30 mm. It becomes practicable to establish the fatigue design curve for each category of joints, by carrying out such analyses on all types of joints.

5. CONCLUSIONS

Parametric analyses on fatigue design curves were carried out under computer simulated variable amplitude stresses covering the stress fluctuations assumed to occur in highway bridges. The fatigue life of four types of welded joints was estimated by the fracture mechanics approach. The principal results obtained from this study are the following:

(1) Fatigue life curves representing the relationship between the equivalent stress range and the crack propagation life under variable amplitude stresses agree to those under constant amplitude stresses

in the shorter life region. However, in the longer life region the curves differ noticeably continuing to decline even below the constant amplitude fatigue limits.

(2) The configuration of fatigue life curves under variable amplitude stresses varies with the traffic constitution and the beam span particularly in the longer life region. As the percentage of large trucks decreases or when the beam span is longer, the equivalent stress range as against the maximum stress range becomes so small that the fatigue life curve is lowered.

(3) It is difficult to define the fatigue limit under variable amplitude stresses for each type of joint by enveloping the group of fatigue life curves estimated under various stress fluctuations.

(4) According to the method of calculating the stress range where the Miner's summation counted from the high stress side using the fatigue life curves estimated under various stress fluctuations reaches one, the fatigue limit under variable amplitude stresses could be defined for each type of joint. In evaluating accurately the fatigue life of steel highway bridge members under actual loadings, it would be practical to apply Miner's rule to the fatigue design curves consisting of a slanting line and a fatigue limit obtained by the method proposed in this study.

REFERENCES

1) Nishikawa, K. : Fatigue Problem and Repair-Rehabilitation of Highway Bridges, The Bridge and Foundation Engineering, Vol. 17, No. 8, pp. 19~23, Aug. 1983 (in Japanese).
2) Subcommittee for Investigation of Fatigue Damage of Steel Structures, Committee for Steel Structures : Survey of Fatigue Damages in Steel Bridges, Proc. of JSCE, No. 368/ I -5, pp. 1~12, Apr. 1984 (in Japanese).
3) Public Works Research Institute : Survey on Technique for Evaluation and Improvement of the Durability of Existing Bridges, Technical Notes of PWRI, The Ministry of Construction, No. 2420, Nov. 1986 (in Japanese).
4) Takenouchi, H., Tanikura, I., Furukawa, M. and Miki, C. : Measurements of Stresses and Deformations of Bridges under Actual Traffic Loadings, Structural Engineering, Vol. 32A, pp. 631~639, Mar. 1986 (in Japanese).
5) Fisher, J. W., Mertz, D. R. and Zhong, A. : Steel Bridge Members under Variable Amplitude Long Life Fatigue Loading, National Cooperative Highway Research Program Report 267, Dec. 1983.
6) JSCE : Standard for Design of Steel Railway Bridges, 1983 (in Japanese).
7) British Standards Institution : BS 5400, Steel Concrete and Composite Bridges, Part 10. Code of Practice for Fatigue, 1979.
8) Europian Convention for Constructional Steelwork Technical Committee 6 : Recommendations for the Fatigue Design of Steel Structures, Publication No. 43, 1985.
9) American Association of State Highway and Transportation Officials : Standard Specifications for Highway Bridges, 1977.
10) Miki, C., Murakoshi, J. and Sakano, M. : Fatigue Crack Growth in Highway Bridges, Structural Eng. /Earthquake Eng., Vol. 4, No. 2, pp. 371 s~380 s, Oct. 1987.
11) Miki, C., Goto, Y., Yoshida, H. and Mori, T. : Computer Simulation Studies on the Fatigue Load and Fatigue Design of Highway Bridges, Proc. of JSCE, Structual Eng. /Earthquake Eng., Vol. 2, No. 1, pp. 13 s~22 s, 1985.
12) Yamada, K. and Hirt, M. A. : Parametric Fatigue Analysis of Weldments Using Fracture Mechanics, Proc. of JSCE, No. 319, pp. 55~64, Mar. 1982 (in Japanese).
13) Honshu-Shikoku Bridges Authority : Code of Steel Plates for Super Structures of Honshu-shikoku Bridges, Mar. 1979 (in Japanese).
14) Okamura, H. : Introduction to Linear Elastic Fracture Mechanics, Baifukan, 1976 (in Japanese).
15) Zettlemoyer, N. and Fisher, J. W. : Stress Gradient Correction Factor for Stress Intensity at Welded Gusset Plates, Welding Journal, p. 59-s, Feb. 1978.

(Received August 24 1987)